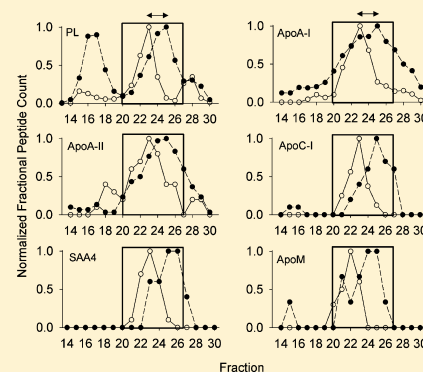# A Comparison of the Mouse and Human Lipoproteome: Suitability of the Mouse Model for Studies of Human Lipoproteins

Scott M. Gordon,[†] Hailong Li,[‡] Xiaoting Zhu,[‡] Amy S. Shah,[§] L. Jason Lu,[‡] and W. Sean Davidson*,[†]

[†]Center for Lipid and Arteriosclerosis Science, Department of Pathology and Laboratory Medicine, University of Cincinnati, 2120 East Galbraith Road, Cincinnati, Ohio 45237-0507, United States

[‡]Division of Biomedical Informatics, Cincinnati Children's Hospital Research Foundation, 3333 Burnet Avenue, MLC 7024, Cincinnati, Ohio 45229-3039, United States

[§]Department of Pediatrics, Cincinnati Children's Hospital Research Foundation, 3333 Burnet Avenue, MLC 7012, Cincinnati, Ohio 45229-3039, United States

S *Supporting Information*

ABSTRACT: Plasma levels of low density lipoproteins (LDL) and high density lipoproteins (HDL) exhibit opposing associations with cardiovascular disease in human populations and mouse models have been heavily used to derive a mechanistic understanding of these relationships. In humans, recent mass spectrometry studies have revealed that the plasma lipoproteome is significantly more complex than originally appreciated. This is particularly true for HDL which contains some 90 distinct proteins, a majority of which play functional roles that go beyond those expected for simple lipid transport. Unfortunately, the mouse lipoproteome remains largely uncharacterized—a significant gap given the heavy reliance on the model. Using a gel filtration chromatography and mass spectrometry analysis that targets phospholipid-bound plasma proteins, we compared the mouse lipoproteome and its size distribution to a previous, identical human analysis. We identified 113 lipid associated proteins in the mouse. In general, the protein diversity in the LDL and HDL size ranges was similar in mice versus humans, though some distinct differences were noted. For the majority of proteins, the size distributions, that is, whether a given protein was associated with large versus small HDL particles, for example, were also similar between species. Again, however, there were clear differences exhibited by a minority of proteins that may reflect metabolic differences between species. Finally, by correlating the lipid and protein size profiles, we identified five proteins that closely track with the major HDL protein, apolipoprotein A-I across both species. Thus, mice have most of the minor proteins identified in human lipoproteins that play key roles in inflammation, innate immunity, proteolysis and its inhibition, and vitamin transport. This provides support for the continued use of the mouse as a model for many aspects of human lipoprotein metabolism.

KEYWORDS: *high density lipoprotein, proteomics, lipoprotein, apolipoprotein, mass spectrometry, mouse model*

INTRODUCTION

Lipoproteins are complexes of lipid emulsified by a diverse set of amphipathic proteins called apolipoproteins, an ingenious solution to the "oil in water" conundrum. In humans and certain genetically modified mice, circulating levels of cholesterol in low density lipoprotein (LDL) are directly related to development of atherosclerosis and subsequent cardiovascular disease (CVD) while levels in high density lipoprotein (HDL) are inversely related.[1] Due to specific sequence and structural features, apolipoproteins mediate on-particle processing of the lipid cargo as well as its targeted delivery throughout the body. Therefore, the "lipoproteome" of a given particle plays a major role in determining its protective or pathological fate, that is, whether lipid is catabolized in the liver or ends up accumulating in a coronary artery, for example.

Our understanding of how protein composition affects lipoprotein metabolism has been hampered because the proteome of these particles is turning out to be remarkably complex. Recent applications of mass spectrometry have shown that human HDL contains nearly 90 distinct proteins,[2−5] any or all of which may impinge on the potentially antiatherogenic functions of this lipoprotein class. These include the "major" proteins like apolipoprotein (apo)A-I and apoA-II which together account for around 70% of total protein mass in ultracentrifugation derived HDL. These are sometimes referred to as scaffold or platform proteins because of their key roles in maintaining HDL particle structure[6] and the possibility that they coordinate the binding of other proteins to the particles.[7,8] However, the numerous "minor" HDL-associated proteins have known functions ranging from lipid transport, innate immunity, coagulation, regulation of the complement system, metal ion

transport, and even glucose metabolism (reviewed in refs 4 and 9). All of these proteins cannot reside on the same particle due to the limited size of human HDL.[10] Work by our laboratory and others has shown that these proteins distribute throughout the HDL family in distinct patterns across particle density,[11−14] size[15,16] and ionic character.[16,17] Thus, in humans, HDL is actually a diverse collection of phospholipid-containing particles that vary in protein composition, and presumably function. The human LDL proteome is less diverse, but still contains >20 distinct proteins in addition to its defining molecule of apolipoprotein (apo)B and these may also be differentially distributed among LDL density subclasses.[18−20] While some LDL proteins play roles in inflammation, most seem directed at lipid transport and control of lipid hydrolysis.

Genetically tractable mouse models have been used extensively in the mechanistic study of lipoprotein metabolism and its link to CVD. However, mice exhibit significant differences in lipid metabolism versus humans. For example, they lack cholesteryl ester transfer protein (CETP),[21] which shuttles cholesteryl esters from HDL to apoB-containing lipoproteins such as LDL and very low density lipoproteins (VLDL) in humans. Thus, mice carry the majority of plasma cholesterol in HDL[22] while humans carry much of it in LDL. This difference has been offered as an explanation for why mice are inherently resistant to the development of atherosclerosis, at least until genetically manipulated (for a review, see ref 23). However, other factors may also play a role in this protection. A better understanding of the proteomic composition of mouse lipoproteins may offer additional explanations and provide a stronger rationale for the use of mice to study human atherosclerotic disease.

Unfortunately, unlike in humans, detailed studies of the mouse lipoproteome are scarce. Puppione and colleagues[24] analyzed UC-isolated mouse HDL from two strains of mice focusing on post-translational modifications of the major apolipoproteins known to be present in HDL. Julve et al.[25] used 2-D gel electrophoresis and mass spectrometry to study the effect of apoA-II overexpression on triglyceride metabolism in mice. They observed that human apoA-II introduction reduced mouse apoA-I, apoC-III, and apoE in HDL in this model. However, we are unaware of a detailed shotgun mass spectrometry analysis of the mouse lipoproteome aimed at detecting more minor protein components, such as those found in human HDL and LDL.

In this work, we examined the mouse plasma lipoproteome and its particle size distribution using a combination of gel filtration chromatography and mass spectrometry. We then compared the results to our previous study of human lipoproteins[15] which used identical methodology. An important consideration in both studies was the use of a calcium silica hydrate (CSH) resin to specifically bind phospholipid-containing particles prior to mass spectrometry. This permitted the analysis of size-separated lipoproteins with minimal interference from large molecular weight or highly abundant lipid-unassociated proteins which may coelute with the lipoproteins.

■ EXPERIMENTAL SECTION

Animal Models and Plasma Collection

All mice used in this study were on the C57BL/6J background and were fed a standard chow diet at all times post weaning. Mice were maintained in American Association for Accred-itation of Laboratory Animal Care approved pathogen-free animal facilities, and the institutional laboratory animal medical services at University of Cincinnati approved all experimental protocols. The mice were between 10 and 32 weeks of age at the time of blood sampling. Blood was collected from ketamine anesthetized mice ($n = 6$) by cardiac puncture using citrate as the anticoagulant. Cellular components were pelleted by centrifugation at ∼$1590g$ for 15 min in a table top centrifuge at room temperature. Plasma was stored at 4 °C until gel filtration separation, always within 16 h. The samples were never frozen.

Plasma Separation by Gel Filtration Chromatography

A volume of 370 μL of plasma from a single mouse was applied to three Superdex 200 gel filtration columns (10/300 GL; GE Healthcare) arranged in series on an ÄKTA FPLC system (GE Healthcare).[15] The sample was separated at a flow rate of 0.3 mL/min in standard Tris buffer (STB) (10 mM Tris, 0.15 M NaCl, 1 mM EDTA). Eluate was collected as 1.5 mL fractions on a Frac 900 fraction collector (GE healthcare) maintained at 4 °C. Each fraction was assessed for choline-containing phospholipid and total cholesterol by colorimetric kits from Wako (Richmond, VA).

Isolation of Phospholipid-Containing Particles Using Calcium Silica Hydrate (CSH)

The fractions were then passed through a calcium silica hydrate (CSH) resin to bind components that contain phospholipid (PL), as previously described.[15] All lipid containing particles tightly associate with the CSH while abundant nonlipid associated proteins are washed through. Briefly, in a 96-well filter plate (Millipore), 45 μg of CSH (from 100 mg/mL stock solution in 50 mM ammonium bicarbonate (AB)) per 1 μg of PL in 400 μL of fraction was mixed gently for 30 min at room temperature. The sample solution was removed by applying a vacuum in a manifold (Millipore) and then washed with 50 mM AB. Lipid-containing proteins that remained associated with the CSH were trypsinized with 1.5 μg of sequencing grade trypsin (Promega) overnight at 37 °C, and the peptides were washed off the resin and into a clean 96 well plate, reduced with dithiothreitol (200 mM; 30 min at 37 °C) and carbamidomethylated with iodoacetamide (800 mM; 30 min at room temperature). The peptides were then vacuum pelleted and stored at −20 °C until MS analysis.

Mass Spectrometry Analysis of Fractions

Dried peptides were reconstituted in 15 μL of 0.1% formic acid in water. An Agilent 1100 series autosampler/HPLC was used to draw 0.5 μL of sample and inject it onto a C18 reverse phase column (GRACE; 150 × 0.500 mm) where an acetonitrile concentration gradient (5−30% in water with 0.1% formic acid) was used to elute peptides for online ESI-MS/MS by a QStar XL mass spectrometer (Applied Biosystems). Pertinent instrument scan settings were as follows: 4800 scans were taken during 140 min of elution for ions between 300 to 1800 m/z with charge states of 2 to 5 exceeding 10 counts. Former target ions were excluded for 300 s. Column cleaning was performed automatically with 2 cycles of a 5−85% acetonitrile gradient lasting 15 min each between runs.

Mass Spectrometry Data Analysis

To identify the protein composition of lipid-containing particles in the various gel filtration fractions, peak lists generated from an analysis of each fraction were scanned against the Swiss-Prot Protein Knowledgebase for *Mus musculus*

(release 2011, 533 657 sequences) using the Mascot (version 2.2.07) and X! Tandem (version 2010.12.01.1) search engines. Search criteria included: variable modifications of Met oxidation and carbamidomethylation, both peptide tolerance and MS/MS tolerance set to ±35 PPM, and up to three missed tryptic cleavage sites allowed. Scaffold software (version Scaffold_4.3.4, Proteome Software) was used to validate MS/MS based peptide and protein identifications. Peptide identification required a value of 99% probability (using data from both Mascot and X!Tandem) using the Peptide Prophet algorithm.[26] Positive protein identification required a value of 95% probability by the Protein Prophet algorithm.[27] Also, a minimum of two peptides were required unless the protein in question was found with single peptide hits in consecutive fractions that were consistent across animal subjects. Since equal volumes of sample were applied to the MS analysis, the relative amount of a given protein present in a given fraction is proportional to the number of spectral counts (i.e., the number of MS/MS spectra assigned to a particular protein) in each fraction. In no case were conclusions made about the relative abundance of two different proteins on the basis of peptide counting. We have previously demonstrated that this approach provides a semiquantitative abundance pattern across each fraction that matches well with patterns derived from immunological analyses.[28]

Apolipoprotein Coshift Analysis

We noticed that phospholipid and apoA-I (and therefore likely the "HDL" particles) eluted earlier in the mouse versus the human plasma samples we have analyzed previously.[15] This offered an opportunity to identify which apolipoproteins track specifically with apoA-I in both species. We developed a novel way to track apolipoprotein elution patterns between the two species which we called a coshift analysis. First, we aimed to identify those apolipoproteins that migrate similarly to apoA-I in both mice and humans. We utilized a Pearson's correlation coefficient (PCC) and subjected them to a Student's t distribution to test the hypothesis of no correlation against the alternative that there is a nonzero correlation to determine the elution similarities between all discovered proteins and apoA-I within each species. Proteins with a PCC ≥ 0.70 and p-value ≤ 0.05 were considered to track with apoA-I in both species. We next identified HDL proteins that shift with apoA-I in the human and mouse system by applying a lag-score (L-score) to reflect where a given protein eluted across the fractions. Apo-A-I was chosen because differences in its structure have been implicated in the differential size distributions of HDL particles in mice and humans (see Discussion). Suppose an abundance profile of a protein P_x is $X = (..., x_r, ...)_r \in [13..30]$, where x_r is the peptide spectral counts of protein P_x in fraction r. With m human and n mouse subjects, L-score L^x of a protein P_x was obtained as

$$L^x = F\left(\frac{1}{\mu}\sum_{i=1}^{m}X_h^i, \frac{1}{\nu}\sum_{j=1}^{n}X_m^j\right)$$

where $\mu = \max(\Sigma_{i=1}^{m}X_h^i)$, $\nu = \max(\Sigma_{j=1}^{n}X_m^f)$, and $X_h^i X_m^f$ are abundance profiles of protein P_x from ith human and jth mouse. $F(f,g)$ is time-lag function calculated with cross-correlation. For discrete functions, the cross-correlation is an array defined as

$$(f*g)[i] \underline{\underline{\text{def}}} \sum_{m=-\infty}^{\infty} f^*[t]g[t+i]$$

where $f^*[t]$ denotes the complex conjugate of f and t is the time lag. Time-lag $F(f,g)$ between two signals is obtained by computing the distance between the center and the maximum position of cross-correlation array. Then, we filtered the proteins with the condition

$$\text{sgn}(L^x) = \text{sgn}(L^{A1})$$

where $\text{sgn}(*)$ is the sign function and L^{A1} is L-score reflecting the shift fractions between human apoA-I and mouse apoA-I. The two constraints were designed to couple together for coshifting protein discovery.

■ RESULTS

Mouse Lipoprotein Size Patterns

Fresh WT C57BL6 mouse plasma was separated by size exclusion chromatography and the collected fractions were assayed for total cholesterol (TC) and phospholipid (PL) content. Figure 1 compares the TC elution profile for mice with
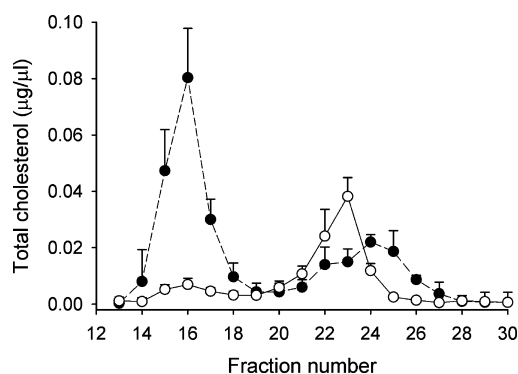

Figure 1. Lipoprotein profiles for mouse and human plasma separated by gel filtration chromatography tracked by total cholesterol. A volume of 370 μL of mouse or human plasma was analyzed on a triple Superdex setup as described in the Experimental Section. Total cholesterol was measured in each fraction by colorimetric assay and plotted versus the fraction number (1.5 mL fractions). Human plasma is represented by closed circles and mouse plasma by open circles. Error bars represent 1 sample standard deviation from $n = 6$ mouse measurements (i.e., 6 individual animals) and $n = 3$ human measurements (3 individual subjects).

that of normolipidimic humans separated using the same system. In previous work,[15] we established that ultra-centrifugally isolated apoB-containing lipoproteins VLDL and LDL elute in the single peak between fractions 14 and 19 (peak 1). Ultracentrifugally isolated HDL particles elute in a broader peak between fractions 20 and 26 (peak 2). Smaller, nonlipid associated proteins elute near the total volume of the system at fractions 27 to 30. (Note: Since our method of separation was based on size and not density, the designations of "HDL" and "LDL", which are based exclusively on density, cannot be appropriately applied to the gel filtration factions reported here. For this Article, we refer to lipids and proteins eluting in the LDL or HDL size range, but we recognize that these may not strictly reflect particles as separated by traditional density ultracentrifugation methods.) Figure 1 confirms that mice carry most of their cholesterol in HDL sized particles with less in the VLDL/LDL range, as shown in dozens of prior FPLC studies (see ref 29 for one of the earliest examples). In contrast, humans carry up to 2/3 of cholesterol in the VLDL/LDL range with the remainder in the HDL size range. The HDL

cholesterol peak from human plasma appeared bimodal, likely reflecting its well-known polydispersity (i.e., HDL_2 and HDL_3; see Discussion). The center of mass of the human HDL TC peak was shifted toward smaller sized particles versus the mouse.

Figure 2 shows the same samples tracked by PL indicating overall similar profiles to TC. The mouse particles in the HDL
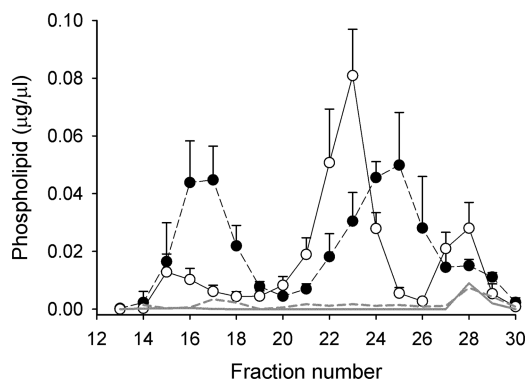

Figure 2. Lipoprotein profiles for mouse and human plasma separated by gel filtration chromatography tracked by phospholipid (PL). The experiment was performed exactly as in Figure 1 except that choline containing phospholipids were measured by enzymatic kit. Human plasma is represented by closed circles and mouse plasma by open circles. Error bars represent 1 sample standard deviation from $n = 6$ mouse measurements (i.e., 6 animals) and $n = 3$ human measurements (3 individual subjects). The gray lines (solid for mouse, dotted for human) show the PL measurement in each fraction after treatment with CSH to select PL-associated proteins.

size range eluted as a tight peak centered at fraction 23, whereas the human particles eluted in a broader peak centered on fraction 25. The bimodality noted in the human TC elution pattern was not as clear in the PL pattern. Unlike in the TC profiles, a third PL peak consistently appeared at fractions 27 and 28 in both species (peak 3). This may be due to lysophospholipids associated with soluble proteins such as albumin which are detected by the choline-based enzymatic assay. Figure 2 also shows that the CSH resin protocol we used was highly effective at adsorbing the PL-containing species from these fractions for the proteomics analysis, as characterized in detail previously.[15]

The Lipoproteome of WT Mice

We evaluated the phospholipid-associated apolipoproteins (i.e., those that bound to the CSH resin after separation by gel filtration, see Experimental Section) in WT mice ($n = 6$). Across all size fractions, 113 separate proteins met our criteria for mass spectrometry based identification. The proteins are listed in Supporting Information Table 1 with the total number of peptides detected for each summed across all fractions. The protein size profiles are shown in the heat map in Figure 3. For each protein, the fraction with the maximum spectral counts was normalized to 1 (red color) and all other fractions scaled accordingly (yellow) and fractions without detectable peptides in blue. This map can be directly compared to Figure 8 in our previous characterization of human plasma.[15] Table 1 shows the 31 PL-associated proteins that we identified in peak 1 (VLDL/LDL size range) and indicates those that have previously been identified in human VLDL[18] or LDL[18−20,30] isolated by ultracentrifugation. In four major proteomic studies of ultracentrifuged LDL from humans (as tracked in the LDL

Proteome Watch[31]), there are 7 proteins which have been identified in all studies (apos B, A-I, C-II, C-III, E, J, and serum amyloid A4) and 15 others that have been found by at least two independent laboratories. We found 12 of these in the LDL/VLDL size range in the mouse (including 5 of the top 7). Surprisingly, we did not detect mouse apoB in this size range (see Discussion for more on this). We also did not find serum amyloid A-4 in the LDL size range, though it was found in abundance in the HDL size range (see below). Additionally, we found several proteins that have not been identified in human LDL including several immunoglobulins including the mouse-specific murinoglobulin and two mannose-binding proteins.

Like humans, most of the proteomic diversity in mouse plasma lipoproteins was found in peak 2 (HDL size range) which was dominated by apoA-I and apoA-II. Of the 103 mouse proteins identified in this region (Table 2), 75 corresponded to a human analogue that has previously been identified in ultracentrifugally isolated HDL according to the HDL Proteome Watch.[5] These include proteins from diverse functional families including lipid transport, coagulation factors, complement factors, anti-inflammatory proteins and protease inhibitors. There were several proteins in the mouse HDL size range that have not yet been identified in centrifugally isolated human HDL including the mouse specific protein murinoglobulin and several members of the IgG family.

Finally, we identified 55 proteins that eluted in peak 3, which we call lipid-poor lipoproteins (Table 3). Many of these overlapped with those in the HDL size range and have previously been identified in UC-isolated HDL. Notable proteins that were not detected in mice in either peaks 2 and 3, but were detected in humans using this same system, included alpha-1-antichymotrypsin, inter-alpha trypsin inhibitor 4, apoD and apoF. This may reflect an overall lower abundance in mice versus humans or issues with the digestion of these proteins on the CSH. Kallistatin, apoL-I, CETP and haptoglobin-related protein were not found as expected due to the lack of these genes in the mouse.

Comparison of Protein Distribution Across Lipoproteins Between Mouse and Human Plasma

We were interested in determining if proteins resided on different size lipoproteins between mice and humans. Albumin, while found in small amounts in ultracentrifugally isolated HDL, is likely a contaminant in this and other studies due to its overwhelming plasma abundance. Figure 4 shows that albumin is primarily found in peak 3 (centered on fractions 27/28) near the total column volume in both species. Human and mouse albumin have similar molecular weights of 66 and 67 kDa, respectively, allowing its use as an internal calibration standard. The fact that albumin exhibited the same elution volume in both species indicates that there were no differences in column resolution or total volume between the human and mouse analyses which were performed months apart. In most cases, the other proteins detected in this study showed no striking difference in elution pattern between the mouse and the human. Of the 113 mouse proteins identified here, 69 had a corresponding human analog and enough distribution data across both species to make a size comparison. Of these, 57 showed no clear difference in the elution pattern using the criteria described in Experimental Section (see Supporting Information Table 1). Some examples are shown in Figure 4. ApoE appeared in large HDL-sized particles in both species as well as in the LDL/VLDL range. The apoE in the HDL range
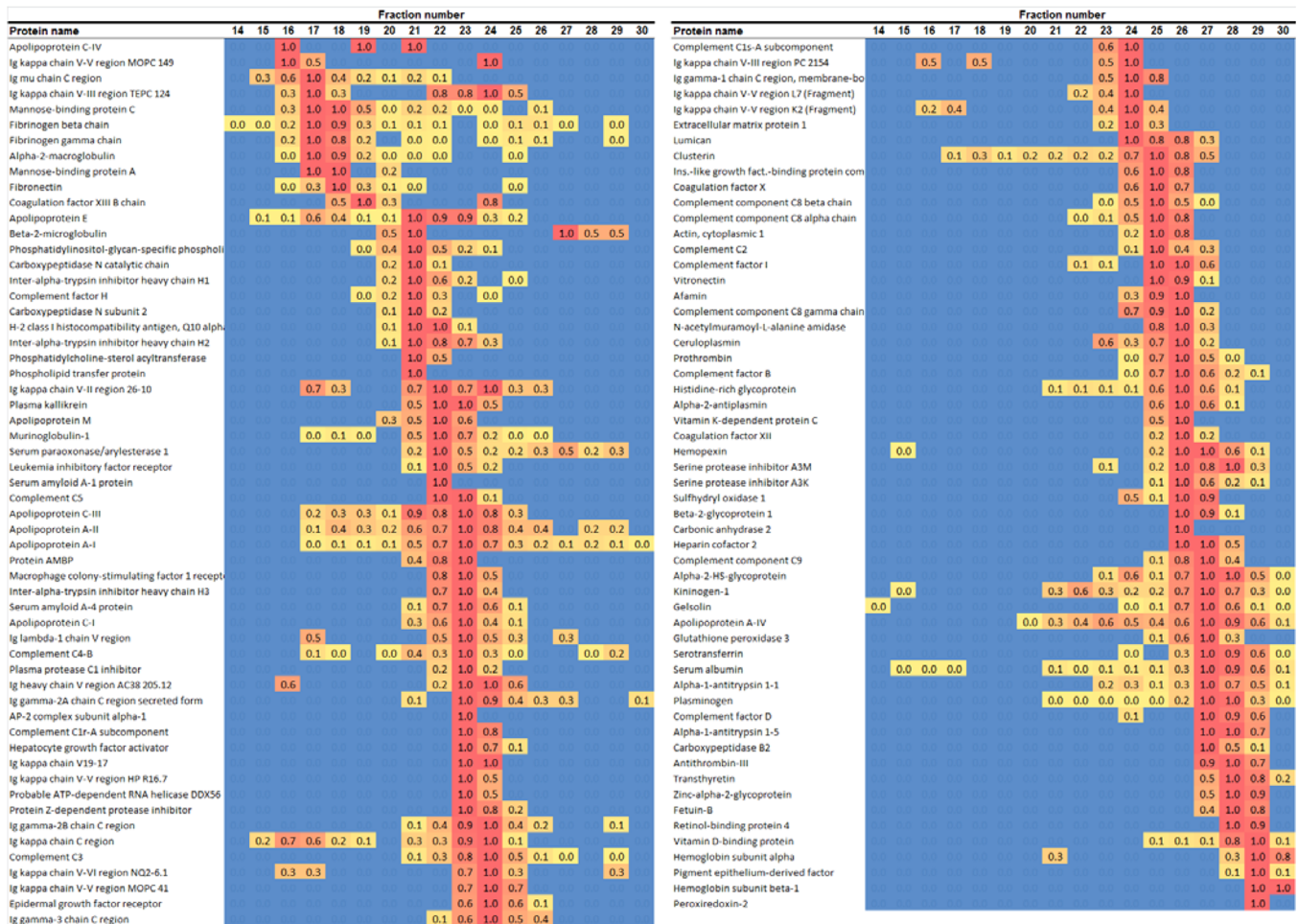
Figure 3. Lipoprotein size distribution profiles for each of the 113 lipid-associated proteins in WT C57BL6 mice. For each gel filtration column fraction, the relative abundance of each identified protein (determined by peptide count) is shown. A value of 1.0 was assigned to the fraction containing the highest peptide count for that particular protein and all other fractions were scaled accordingly. The relative abundance can be assessed by the color of the square with blue equating to 0 detected peptides and red representing the highest number. The list was sorted with respect to peak position with largest proteins at the top left progressing to smallest at the bottom right.

Table 1. Proteins Detected in Peak 1 of the Mouse Lipoproteome, VLDL/LDL Size Range

alpha-2-macroglobulin[a]	fibrinogen beta chain	Ig kappa chain V−VI region NQ2-6.1
apolipoprotein A-I*[b]	**fibrinogen gamma chain***	Ig kappa chain V−V region MOPC 149
apolipoprotein A-II*	fibronectin	Ig lambda-1 chain V region
apolipoprotein C-II*	gelsolin	Ig mu chain C region
apolipoprotein C-III*	hemopexin	kininogen-1
apolipoprotein C-IV*	Ig heavy chain V region AC38 205.12	mannose-binding protein A
apolipoprotein E*	**Ig kappa chain C region***	mannose-binding protein C
clusterin (ApoJ)*	Ig kappa chain V−II region 26−10	murinoglobulin-1
coagulation factor XIII B chain	Ig kappa chain V−III region PC 2154	phosphatidylinositol-glycan-specific phospholipase D
complement C4-B*	Ig kappa chain V−III region TEPC 124	**serum albumin***
complement factor H*	Ig kappa chain V−V region K2	

[a]Proteins in *italic* were not previously identified in human LDL or VLDL isolated by density gradient ultracentrifugation according to the LDL Proteome Watch.[31] [b]Proteins in **bold** with an asterisk (*) were previously identified by at least two independent laboratories identified in human LDL or VLDL isolated by density gradient ultracentrifugation according to the LDL Proteome Watch.[31]

was largely superimposable, suggesting that apoE associates with similarly sized HDL particles in both species. We did note differences for apoE in the LDL/VLDL range with human apoE showing up in larger particles in peak 1 versus the mouse. This is likely due to the increased presence of VLDL in humans versus mice, a well-known repository for apoE. Since this column system is not optimized for separating LDL from VLDL, the leftward shift for apoE in the human samples is consistent with VLDL association. Comparable results were obtained for complement C3 which showed similar distributions in the HDL-size range and a similar VLDL/LDL pattern difference as apoE. PLTP showed an identical profile in both species.

Table 2. Proteins Detected in Peak 2 of the Mouse Lipoproteome, HDL Size Range

actin, cytoplasmic[a]	complement C9*	ins.-like growth fact.-binding protein complex acid labile sub
afamin*[b]	complement factor B*	inter-alpha-trypsin inhibitor H1*
alpha-1-antitrypsin 1-1*	complement factor D	inter-alpha-trypsin inhibitor H2*
alpha-2-antiplasmin*	Complement factor I	inter-alpha-trypsin inhibitor H3
alpha-2-HS-glycoprotein*	epidermal growth factor receptor	kininogen-1*
alpha-2-macroglobulin*	extracellular matrix protein 1	leukemia inhib. factor receptor
AP-2 complex subunit alpha-1[c]	fibrinogen beta chain*	lumican*
apolipoprotein A-I*	fibrinogen gamma chain*	macrophage colony-stimulating factor 1 receptor
apolipoprotein A-II*	fibronectin*	mannose-binding protein A
apolipoprotein A-IV*	gelsolin*	mannose-binding protein C
apolipoprotein C−I*	glutathione peroxidase 3	murinoglobulin-1
apolipoprotein C−II*	H-2 class I histocompatibility antigen, Q10 alpha chain	N-acetylmuramoyl-L-alanine amidase
apolipoprotein C−III*	hemoglobin subunit alpha*	LCAT*
apolipoprotein C−IV*	hemopexin*	PI-glycan-specific PLD*
apolipoprotein E*	heparin cofactor 2*	phospholipid transfer protein*
Apolipoprotein M*	hepatocyte growth factor activator	plasma kallikrein*
beta-2-glycoprotein 1 (apoH)*	histidine-rich glycoprotein*	plasma protease C1 inhibitor*
beta-2-microglobulin	Ig gamma-1 chain C region*	plasminogen*
carbonic anhydrase 2	Ig gamma-2A chain C region	probable ATP-dependent RNA helicase DDX56
carboxypeptidase N cat.	Ig gamma-2B chain C region	protein AMBP*
carboxypeptidase N sub. 2	Ig gamma-3 chain C region	protein Z-dependent protease inhibitor
ceruloplasmin*	Ig heavy chain V region AC38 205.12	prothrombin*
clusterin (apoJ)*	Ig kappa chain C region*	serine protease inhibitor A3K
coagulation factor X	Ig kappa chain V19−17	serine protease inhibitor A3M
coagulation factor XII	Ig kappa chain V−II region 26−10	serotransferrin*
coagulation factor XIII B chain	Ig kappa chain V−III region PC 2154	albumin*
complement C1r-A	Ig kappa chain V−III region TEPC 124	serum amyloid A-1*
complement C 1s-A*	Ig kappa chain V−V region HP R16.7	serum amyloid A-4*
complement C2*	Ig kappa chain V−V region K2	serum paraoxonase 1*
complement C3*	Ig kappa chain V−V region L7	sulfhydryl oxidase 1
complement C4-B*	Ig kappa chain V−V region MOPC 149	vitamin D-binding protein
complement C5	Ig kappa chain V−V region MOPC 41	vitamin K-dependent protein C
complement C8 alpha	Ig kappa chain V−VI region NQ2-6.1	vitronectin*
complement C8 beta	Ig lambda-1 chain V region	
complement C8 gamma chain	Ig mu chain C region	

[a]Proteins in **bold** were previously identified in human HDL isolated by density gradient ultracentrifugation according to the HDL Proteome Watch,[5,31] but not by three or more independent laboratories (putative identifications). [b]Proteins in **bold** with an asterisk (*) were previously identified in human HDL isolated by density gradient ultracentrifugation according to the HDL Proteome Watch[5,31] by three or more independent laboratories (confident identifications). [c]Proteins in *italic* have not been previously identified in human HDL isolated by density gradient ultracentrifugation according to the HDL Proteome Watch.[5,31]

We also noticed proteins that showed an overall similar profile, but with a different distribution of protein between two separate peaks. For example, in both species, apoA-IV was present in a peak centered on fraction 23 and another centered on fraction 28. These likely represent HDL-bound and lipid-poor forms of the protein, respectively. However, the distribution of apoA-IV between the two peaks was about equal in the mice but weighted heavily toward lipid-poor in the human. ApoJ on the other hand, was also distributed between two peaks centered on fractions 20 and 25. In this case, human apoJ was preferentially distributed toward the larger particles but clearly preferred smaller particles in the mouse.

We also found 13 examples of proteins that associated with different size lipoproteins between mice and humans. Two striking examples are complement C1r and LCAT (Figure 5). In both cases, the protein eluted in large particles in humans and smaller particles in the mouse, with no overlap. Other proteins such as Pon1 and A1AT exhibited more complicated patterns that differed in overall shape, but had regions of overlap. Human A1AT associated with particles in the large HDL size range and in a lipid-poor size range whereas the

mouse form primarily exists in the lipid-poor region. SAA1 was also found in quite different sized species, though the number peptides detected was low and should be confirmed with more sensitive techniques.

Finally, we also noticed proteins that appeared to track closely with differences in the PL profile between both species (Figure 6). For these proteins, the center of the peak was shifted to the right for humans and to the left for mice, mirroring differences in the PL profile. These shifts may be indicative of proteins that track with apoA-I mediated changes in particle size (see below).

■ DISCUSSION

The mouse model has been heavily used as an experimental system for the study of lipoprotein metabolism and atherosclerotic disease with an eye toward translation to humans. Thus, it is important to know if the diversity of the mouse lipoprotein proteome is as extensive as that in humans. This is particularly important for HDL which is the most compositionally and functionally complex. The results reported

Table 3. Proteins Detected in Peak 3 of the Mouse Lipoproteome, Lipid Poor Lipoproteins

alpha-1-antitrypsin 1-1*[a]	Complement C9*	lumican*
alpha-1-antitrypsin 1-5*	complement factor B*	N-acetylmuramoyl-L-Ala amidase*
alpha-2-antiplasmin*	complement factor D	Peroxiredoxin-2
Alpha-2-HS-glycoprotein*	complement factor I	pigment epithelium-der. factor*
antithrombin-III*	fetuin-B	plasminogen*
apolipoprotein A-I*	fibrinogen beta chain*	prothrombin*
apolipoprotein A-II*	fibrinogen gamma chain*	retinol-binding protein 4*
apolipoprotein A-IV*	gelsolin*	serine protease inhibitor A3K
beta-2-glycoprotein 1 (apoH)*	glutathione peroxidase 3	serine protease inhibitor A3M
beta-2-microglobulin[b]	hemoglobin subunit alpha*	serotransferrin*
carboxypeptidase B2	hemoglobin subunit beta*	serum albumin*
ceruloplasmin*	hemopexin	serum paraoxonase 1*
clusterin (apoJ)*	heparin cofactor 2	sulfhydryl oxidase 1
coagulation factor XII	histidine-rich glycoprotein	transthyretin*
complement C2*	Ig gamma-2A chain C region	vitamin D binding protein*
complement C3*	Ig gamma-2B chain C region	vitronectin*
complement C4-B*	Ig kappa chain V−VI region NQ2-6.1	zinc-alpha-2-glycoprotein*
complement C8 beta chain	Ig lambda-1 chain V region	
complement C8 gamma chain[c]	kininogen-1*	

[a]Proteins in **bold** with an asterisk (*) were previously identified in human HDL isolated by density gradient ultracentrifugation according to the HDL Proteome Watch[5,31] by three or more independent laboratories (confident identifications). [b]Proteins in **bold** were previously identified in human HDL isolated by density gradient ultracentrifugation according to the HDL Proteome Watch,[5,31] but not by three or more independent laboratories (putative identifications). [c]Proteins in *italics* have not been previously identified in human HDL isolated by density gradient ultracentrifugation according to the HDL Proteome Watch.[5,31]
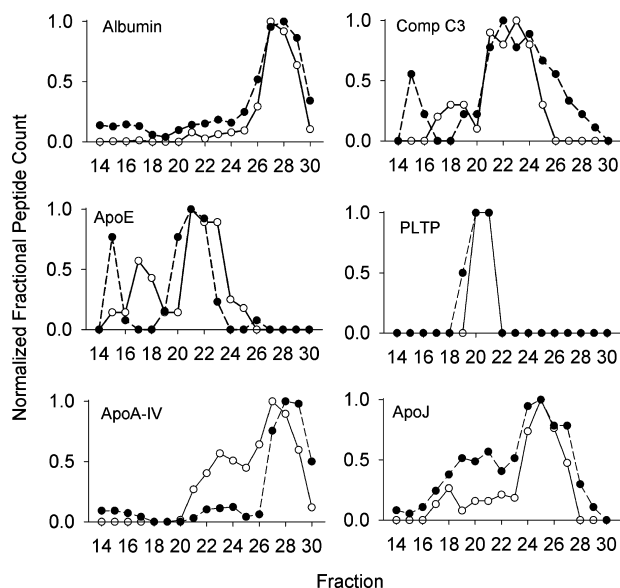

Figure 4. Examples of identified proteins that do not exhibit a noticeable difference in elution profile between mouse and human. The normalized peptide counts (determined as in Figure 3) for the indicated protein across each fraction are shown. For all figures, WT mouse data is represented by open circles and human data is shown in closed circles. Data represents a mean peptide count from 6 mice or 3 humans.

Figure 5. Examples of identified proteins that differ in size distribution between mouse and human. The normalized peptide counts (determined as in Figure 3) for the indicated protein across each fraction are shown. For all figures, WT mouse data is represented by open circles and human data is shown in closed circles. Data represents a mean peptide count from 6 mice or 3 humans.

here indicate that, aside from a handful of primate-specific proteins such as apoL-I, kallistatin, apoprotein(a) and haptoglobin-related protein, most of the same proteins that have been reported in human LDL and HDL also reside in the corresponding mouse lipoproteins. This includes most of the classic "apo" proteins such as apoA-I, A-II, A-IV, E, M, and the C's which are well-known to perform functions related to plasma lipid transport. Additionally, mice also have most of the minor proteins that play roles in inflammation, innate
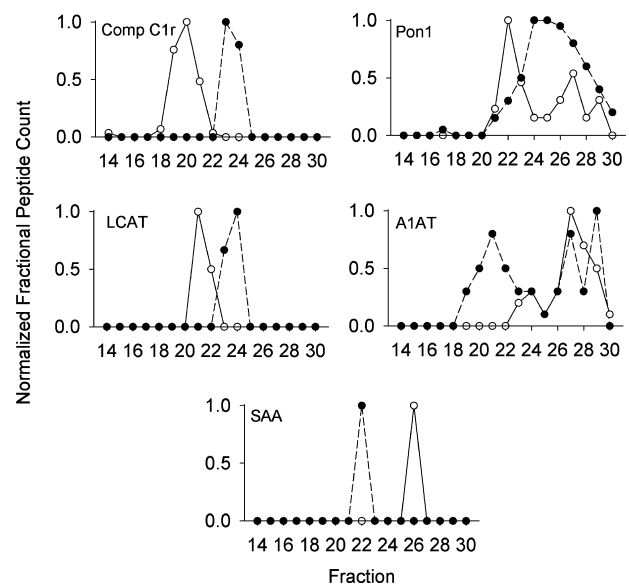
immunity, proteolysis and its inhibition, and vitamin transport. Thus, it seems reasonable to hypothesize that many of the putative protective effects postulated for human HDL may also carry over to mice, both in terms of cardiovascular and noncardiovascular functions. However, their presence in the mouse lipoproteome does not mean that they work the same way in humans and careful validation and functional comparisons must still be performed on a case by case basis.

In each of the different lipoprotein size ranges in the mice, we identified new proteins that had not previously been
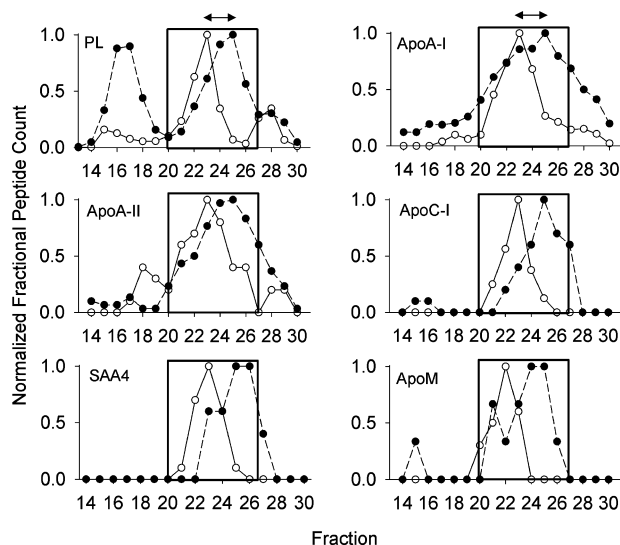
Figure 6. Proteins that are uniformly shifted along with the PL profile between species. Upper left: The phospholipid distribution from Figure 2 is shown normalized to the peak fraction (set to 1). All other panels show the normalized peptide counts (determined as in Figure 3) for the indicated protein across each fraction. The box shows the HDL-size range and the arrows show the consistent size difference between species. For all figures, WT mouse data is represented by open circles and human data is shown in closed circles. Data represents a mean peptide count from 6 mice or 3 humans.

observed in the corresponding human lipoprotein. At this point, these should be thought of as putative identifications that need to be validated with complementary methods. Although the CSH resin is selective for PL-associated proteins, there is a possibility that some proteins associate with the resin in a PL independent fashion. Also, given the sensitivity of modern mass spectrometers and the high concentrations of many plasma proteins, it is possible that some were not completely eliminated during the resin wash steps. Albumin is a good example. The CSH can eliminate upward of 95% of free albumin from human plasma samples.[15] However, given that albumin can reach 50−65 mg/mL in plasma, even a few percent carry-over is readily detectable by mass spectrometry. The best way to address these issues is to compile data from independent laboratories. In the human, some 14 shotgun mass spectrometry studies have identified nearly 224 proteins in HDL, but only 89 of these have been reproduced in at least three independent laboratories.[5] We suggest a similar approach to drive consensus on the mouse lipoproteome.

Most of the mouse proteins found in this study were similarly distributed between lipoprotein classes irrespective of species. For the LDL size range, proteins that typically associate with LDL in humans also tend to associate with LDL in mice. One glaring exception was the surprising failure to find even a single peptide for mouse apoB, the defining apolipoprotein in LDL, even though many immunological studies have demonstrated its presence in mice. Indeed, apoB peptides were readily detectable in humans in the LDL size range.[15] The reason for this is unclear but may arise from the overall low levels of apoB-containing lipoproteins in chow fed mice (which had also been fasted) and the difficulty of proteolysis, and subsequent peptide release, of apoB derived peptides from LDL when it is bound to the CSH resin.

For the HDL size range, there was also high concordance in terms of size distribution between the species for most of the

identified proteins. There were, however, several cases of proteins that differed. For example, LCAT seemed to be associated with significantly larger HDL particles in mice than in humans. This may be related to the lack of CETP and the accumulation of larger CE-rich HDL particles in the mice. It may also be that inherent differences in mouse LCAT or apoA-I sequence tend to favor association with larger particles. ApoA-IV was found to be primarily lipid-poor in humans with only a minor fraction migrating in the HDL range, consistent with previous studies.[32,33] On the other hand, mouse apoA-IV was approximately equally distributed between a medium sized HDL-like particle and the lipid-poor fraction, also consistent with previous studies—at least in rats.[34,35] This may be due to the fact that rodent apoA-IV has an overall higher hydrophobicity than its human counterpart and thus should be more prone to lipid association.[36] The molecular basis for other differences in particle size distribution between the species (i.e., Pon1, A1AT, SAA, etc.) cannot be determined from these studies, but further work may reveal important structural and functional implications that may help explain why WT mice are so robustly protected from CAD.

HDL particles exhibit different size patterns in mouse versus human plasma. Humans have a polymodal distribution, primarily composed of larger HDL_2 (roughly 2/3) and smaller HDL_3 particles (roughly 1/3) as separated by density ultracentrifugation nondenaturing gradient gel electrophoresis and other methods.[37] Mice, on the other hand, exhibit a unimodal distribution centered around 10.2 nm in diameter.[38,39] This observation is widely thought to be due to differences in apoA-I structure because (a) transgenic introduction of human apoA-I into mice completely converted the unimodal mouse profile to a polymodal, humanlike profile[39] and (b) alteration of a specific helical junction in human apoA-I to that resembling mouse apoA-I alters apoA-I's affinity for small versus large HDL.[40]

When closely examining the peptide count profile of apoA-I in mice, we noticed a tight correlation between the patterns of apoA-I and the phospholipid concentration in the HDL size range. This same correlation was present in the human profile, but it was shifted to a smaller size than in the mouse. This is illustrated in Figure 6. If one assumes that differences in apoA-I structure between the two species are responsible for the size shift, then this offers an opportunity to identify which apolipoproteins track along with apoA-I in both species. First, we identified those apolipoproteins that migrate similarly to apoA-I in both mice and humans (see Experimental Section). Then we searched for other proteins that shift in the same direction and magnitude as apoA-I and phospholipid between the human and mouse system. Figure 6 shows the 5 proteins that met the criteria. One interpretation is that these proteins prefer to associate with HDL particles that contain an apoA-I structural scaffold while the others may associate more with other proteins or lipids. The colocalization of apoA-I and apoA-II is well-known; HDL particles containing both apolipoproteins (LpA-I/A-II) can be separated by immunoaffinity chromatography from those that contain apoA-I without apoA-II (LpA-I), but both populations have a similar size distribution.[13] ApoC-I, apoM and apoA-II scored high in their ability to comigrate with apoA-I when human plasma is fractionated by three orthogonal separation techniques,[17] supporting their affinity for apoA-I containing HDL particles. The reason for this association cannot be determined from these studies, but could be due to direct protein−protein

interactions with apoA-I. Alternatively, the association may arise because the characteristics of the lipid surface generated by apoA-I solubilization (i.e., surface curvature, lipid packing density, etc.) may favor their association. Perhaps more interesting was that many (in fact most) of the HDL-associated proteins did not strictly track with apoA-I size shifts between the two species. For example, the fact that apoE failed to demonstrate this shift may indicate that it exists on particles that are largely devoid of apoA-I. This idea was suggested previously by Asztalos et al.[41] who noticed that apoE and apoA-I did not overlap on their 2-D gel separation of human plasma. Further experiments using techniques like immunoprecipitation will be required to determine the colocalization of proteins on the same lipoprotein particles. In addition, since the mouse lipoproteome generally mirrors the human, one can envision taking advantage of the model by knocking out the major scaffold proteins such as apoA-I, apoA-II, and apoA-IV to determine the impact on the levels and size distributions of the minor HDL-associated factors. This work is currently ongoing in our laboratory.

CONCLUSION

In conclusion, we show that the mouse exhibits protein diversity across the LDL and HDL size ranges that is generally similar to that in humans. This bolsters the rationale for use of the mouse model in human studies of the lipoproteome and perhaps to lipoprotein metabolism in general.

ASSOCIATED CONTENT

Ⓢ Supporting Information

(1) Text file containing a list of all proteins identified, their accession numbers, and the total peptide counts found for each. (2) Excel spreadsheet file containing data for all proteins identified and their peptide count distributions across each fraction for each mouse analyzed. The Supporting Information is available free of charge on the ACS Publications website at DOI: 10.1021/acs.jproteome.5b00213.

AUTHOR INFORMATION

Corresponding Author

*Telephone: 513-558-3707. Fax: 513-558-1312. E-mail: Sean. Davidson@uc.edu.

Notes

The authors declare no competing financial interest.

ACKNOWLEDGMENTS

ABBREVIATIONS

Apo, apolipoprotein; CVD, cardiovascular disease; CSH, calcium silica hydrate; HDL, high density lipoprotein; HDL-C, high density lipoprotein cholesterol; LDL, low density lipoprotein; MS, mass spectrometry; PL, phospholipid; STB, standard Tris buffer; UC, ultracentrifugation; VLDL, very low density lipoprotein; WT, wild-type

REFERENCES

(1) Kannel, W. B.; Castelli, W. P.; Gordon, T. Cholesterol in the prediction of atherosclerotic disease. New perspectives based on the Framingham study. *Ann. Int. Med.* **1979**, *90*, 85−91.

(2) Vaisar, T.; Pennathur, S.; Green, P. S.; Gharib, S. A.; Hoofnagle, A. N.; Cheung, M. C.; Byun, J.; Vuletic, S.; Kassim, S.; Singh, P.; et al. Shotgun proteomics implicates protease inhibition and complement activation in the antiinflammatory properties of HDL. *J. Clin. Invest.* **2007**, *117*, 746−756.

(3) Karlsson, H.; Leanderson, P.; Tagesson, C.; Lindahl, M. Lipoproteomics II: mapping of proteins in high-density lipoprotein using two-dimensional gel electrophoresis and mass spectrometry. *HDL Compos.* **2005**, *5*, 1431−1445.

(4) Shah, A. S.; Tan, L.; Lu, L. J.; Davidson, W. S. The proteomic diversity of high density lipoproteins: Our emerging understanding of its importance in lipid transport and beyond. *J. Lipid Res.* **2013**, *54*, 2575−2585.

(5) Davidson, W. S. *The HDL Proteome Watch*; 2015; http://homepages.uc.edu/~davidswm/HDLproteome.html.

(6) Phillips, M. C. New insights into the determination of HDL structure by apolipoproteins: Thematic review series: High density lipoprotein structure, function, and metabolism. *J. Lipid Res.* **2013**, *54*, 2034−2048.

(7) Huang, Y.; Wu, Z.; Riwanto, M.; Gao, S.; Levison, B. S.; Gu, X.; Fu, X.; Wagner, M. A.; Besler, C.; Gerstenecker, G.; et al. Myeloperoxidase, paraoxonase-1, and HDL form a functional ternary complex. *J. Clin. Invest.* **2013**, *123*, 3815−3828.

(8) Shiflett, A. M.; Bishop, J. R.; Pahwa, A.; Hajduk, S. L. Human high density lipoproteins are platforms for the assembly of multi-component innate immune complexes. *J. Biol. Chem.* **2005**, *280*, 32578−32585.

(9) Heinecke, J. W. The HDL proteome: A marker—and perhaps mediator—of coronary artery disease. *J. Lipid Res.* **2009**, *50* (Suppl), S167−S171.

(10) Kostner, G.; Alaupovic, P. Studies of the composition and structure of plasma lipoproteins. Separation and quantification of the lipoprotein families occurring in the high density lipoproteins of human plasma. *Biochemistry* **1972**, *11*, 3419−3428.

(11) Davidson, W. S.; Silva, R. A. G. D.; Chantepie, S.; Lagor, W. R.; Chapman, M. J.; Kontush, A. Proteomic Analysis of Defined HDL Subpopulations Reveals Particle-Specific Protein Clusters: Relevance to Antioxidative Function. *Arterioscler., Thromb., Vasc. Biol.* **2009**, *29*, 870−876.

(12) Coetzee, G. A.; Strachan, A. F.; van der Westhuyzen, D. R.; Hoppe, H. C.; Jeenah, M. S.; de Beer, F. C. Serum amyloid A-containing human high density lipoprotein 3. Density, size, and apolipoprotein composition. *J. Biol. Chem.* **1986**, *261*, 9644−9651.

(13) Cheung, M. C.; Albers, J. J. Characterization of lipoprotein particles isolated by immunoaffinity chromatography. Particles containing A-I and A-II and particles containing A-I but no A-II. *J. Biol. Chem.* **1984**, *259*, 12201−12209.

(14) Cheung, M. C.; Albers, J. J. Distribution of high density lipoprotein particles with different apoprotein composition: particles with A-I and A-II and particles with A-I but no A-II. *J. Lipid Res.* **1982**, *23*, 747−753.

(15) Gordon, S. M.; Deng, J.; Lu, L. J.; Davidson, W. S. Proteomic characterization of human plasma high density lipoprotein fractionated by gel filtration chromatography. *J. Proteome Res.* **2010**, *9*, 5239−5249.

(16) Asztalos, B. F.; Schaefer, E. J. High-density lipoprotein subpopulations in pathologic conditions. *Am. J. Cardiol.* **2003**, *91*, 12E−17E.

(17) Gordon, S. M.; Deng, J.; Tomann, A. B.; Shah, A. S.; Lu, L. J.; Davidson, W. S. Multi-dimensional co-separation analysis reveals protein:protein interactions defining plasma lipoprotein subspecies. *Mol. Cell. Proteomics* **2013**, *12*, 3123−3134.

(18) Dashty, M.; Motazacker, M. M.; Levels, J.; de, V. M.; Mahmoudi, M.; Peppelenbosch, M. P.; Rezaee, F. Proteome of human plasma very low-density lipoprotein and low-density lip-

oprotein exhibits a link with coagulation and lipid metabolism. *Thromb. Haemostasis* **2014**, *111*, 518−530.

(19) Karlsson, H.; Leanderson, P.; Tagesson, C.; Lindahl, M. Lipoproteomics I: mapping of proteins in low-density lipoprotein using two-dimensional gel electrophoresis and mass spectrometry. *Proteomics* **2005**, *5*, 551−565.

(20) Stahlman, M.; Davidsson, P.; Kanmert, I.; Rosengren, B.; Boren, J.; Fagerberg, B.; Camejo, G. Proteomics and lipids of lipoproteins isolated at low salt concentrations in D_2O/sucrose or in KBr. *J. Lipid Res.* **2008**, *49*, 481−490.

(21) Guyard-Dangremont, V.; Desrumaux, C.; Gambert, P.; Lallemant, C.; Lagrost, L. Phospholipid and cholesteryl ester transfer activities in plasma from 14 vertebrate species. Relation to atherogenesis susceptibility. *Comp. Biochem. Physiol., Part B: Biochem. Mol. Biol.* **1998**, *120*, 517−525.

(22) Camus, M. C.; Chapman, M. J.; Forgez, P.; Laplaud, P. M. Distribution and characterization of the serum lipoproteins and apoproteins in the mouse, Mus musculus. *J. Lipid Res.* **1983**, *24*, 1210−1228.

(23) Getz, G. S.; Reardon, C. A. Animal Models of Atherosclerosis. *Arterioscler., Thromb., Vasc. Biol.* **2012**, *32*, 1104.

(24) Puppione, D. L.; Yam, L. M.; Bassilian, S.; Souda, P.; Castellani, L. W.; Schumaker, V. N.; Whitelegge, J. P. Mass spectral analysis of the apolipoproteins on mouse high density lipoproteins. Detection of post-translational modifications. *Biochim. Biophys. Acta* **2006**, *1764*, 1363−1371.

(25) Julve, J.; Escola-Gil, J. C.; Rotllan, N.; Fievet, C.; Vallez, E.; de la Torre, C.; Ribas, V.; Sloan, J. H.; Blanco-Vaca, F. Human apolipoprotein A-II determines plasma triglycerides by regulating lipoprotein lipase activity and high-density lipoprotein proteome. *Arterioscler., Thromb., Vasc. Biol.* **2010**, *30*, 232−238.

(26) Keller, A.; Nesvizhskii, A. I.; Kolker, E.; Aebersold, R. Empirical statistical model to estimate the accuracy of peptide identifications made by MS/MS and database search. *Anal. Chem.* **2002**, *74*, 5383−5392.

(27) Nesvizhskii, A. I.; Keller, A.; Kolker, E.; Aebersold, R. A statistical model for identifying proteins by tandem mass spectrometry. *Anal. Chem.* **2003**, *75*, 4646−4658.

(28) Davidson, W. S.; Silva, R. A.; Chantepie, S.; Lagor, W. R.; Chapman, M. J.; Kontush, A. Proteomic analysis of defined HDL subpopulations reveals particle-specific protein clusters: relevance to antioxidative function. *Arterioscler., Thromb., Vasc. Biol.* **2009**, *29*, 870−876.

(29) Jiao, S.; Cole, T. G.; Kitchens, R. T.; Pfleger, B.; Schonfeld, G. Genetic heterogeneity of lipoproteins in inbred strains of mice: analysis by gel-permeation chromatography. *Metabolism* **1990**, *39*, 155−160.

(30) Bancells, C.; Canals, F.; Benitez, S.; Colome, N.; Julve, J.; Ordonez-Llanos, J.; Sanchez-Quesada, J. L. Proteomic analysis of electronegative low-density lipoprotein. *J. Lipid Res.* **2010**, *51*, 3508−3515.

(31) Davidson, W. S. *The LDL Proteome Watch*; 2015; http://homepages.uc.edu/~davidswm/LDLproteome.html.

(32) Bisgaier, C. L.; Sachdev, O. P.; Megna, L.; Glickman, R. M. Distribution of apolipoprotein A-IV in human plasma. *J. Lipid Res.* **1985**, *26*, 11−25.

(33) Lambert, G.; Chase, M. B.; Dugi, K.; Bensadoun, A.; Brewer, H. B. J.; Santamarina-Fojo, S. Hepatic lipase promotes the selective uptake of high density lipoprotein-cholesteryl esters via the scavenger receptor B1. *J. Lipid Res.* **1999**, *40*, 1294−1303.

(34) DeLamatre, J. G.; Hoffmeier, C. A.; Lacko, A. G.; Roheim, P. S. Distribution of apolipoprotein A-IV between the lipoprotein and the lipoprotein-free fractions of rat plasma: Possible role of lecithin:cholesterol acyltransferase. *J. Lipid Res.* **1983**, *24*, 1578−1585.

(35) Fidge, N. H. The redistribution and metabolism of iodinated apolipoprotein A-IV in rats. *Biochim. Biophys. Acta* **1980**, *619*, 129−141.

(36) Weinberg, R. B. Differences in the hydrophobic properties of discrete alpha-helical domains of rat and human apolipoprotein A-IV. *Biochim. Biophys. Acta* **1987**, *918*, 299−303.

(37) Lindgren, F. T.; Elliot, H. A.; Gofman, J. W. The ultracentrifugal characterization and isolation of human blood lipids and lipoproteins, with applications to the study of atherosclerosis. *J. Phys. Colloid Chem.* **1951**, *55*, 80−93.

(38) Chajek-Shaul, T.; Hayek, T.; Walsh, A.; Breslow, J. L. Expression of the human apolipoprotein A-I gene in transgenic mice alters high density lipoprotein (HDL) particle size distribution and diminishes selective uptake of HDL cholesteryl esters. *Proc. Natl. Acad. Sci. U. S. A* **1991**, *88*, 6731−6735.

(39) Rubin, E. M.; Ishida, B. Y.; Clift, S. M.; Krauss, R. M. Expression of human apolipoprotein A-I in transgenic mice results in reduced plasma levels of murine apolipoprotein A-I and the appearance of two new high density lipoprotein size subclasses. *Proc. Natl. Acad. Sci. U. S. A.* **1991**, *88*, 434−438.

(40) Carnemolla, R.; Ren, X.; Biswas, T. K.; Meredith, S. C.; Reardon, C. A.; Wang, J.; Getz, G. S. The specific amino acid sequence between helices 7 and 8 influences the binding specificity of human apolipoprotein A-I for high density lipoprotein (HDL) subclasses: A potential for HDL preferential generation. *J. Biol. Chem.* **2008**, *283*, 15779−15788.

(41) Santos, R. D.; Schaefer, E. J.; Asztalos, B. F.; Polisecki, E.; Wang, J.; Hegele, R. A.; Martinez, L. R.; Miname, M. H.; Rochitte, C. E.; Da Luz, P. L.; et al. Characterization of high density lipoprotein particles in familial apolipoprotein A-I deficiency. *J. Lipid Res.* **2008**, *49*, 349−357.